

Effects of rattan fiber length variation on mechanical properties, characterization, and microstructure of concrete

Andi Yusra^{*1, a}, Zakia^{1, b}, Surya Perdana^{1, c}, Fachruddin Fachruddin^{1, d}, Teuku Budi Aulia^{2, e}

¹Department of Civil Engineering, Teuku Umar University, Meulaboh, Indonesia

²Department of Civil Engineering, Syiah Kuala University, Banda Aceh, Indonesia

Article Info

Abstract

Article history:

Received 05 Mar 2024

Accepted 31 May 2024

Keywords:

Microstructure;
Characterization;
Fiber concrete;
Concrete strength

The study aimed to test how variations in fiber length affect the behavior of microstructures in concrete, as well as to characterize and analyze their mechanical properties. This research covers several specific objectives, including understanding the influence of different fiber lengths on micro and macrostructural aspects of concrete, assessing the mechanical properties of reinforced concrete with fibers of various lengths, and examining the relationship between fiber length and the mechanical performance of concrete. The results showed that the addition of rattan fibers in concrete can increase or even reduce tensile strength depending on the length of the fibers and their material characteristics. The addition of rattan fibers with a length of 30 mm results in a significant increase in tensile strength, while longer or shorter fiber lengths do not yield equally favorable results. Analysis of the chemical composition of concrete shows that the elements oxygen (O), calcium (Ca), and silicon (Si) predominate, with the addition of carbon (C), iron (Fe), aluminum (Al), magnesium (Mg), and Sulphur (S) elements in concrete with rattan fibers. Morphological observations using SEM on concrete, both with fibers and without fibers, provide an in-depth understanding of the structure of concrete surfaces microscopically.

© 2024 MIM Research Group. All rights reserved.

1. Introduction

Concrete is a widely utilized construction material due to its exceptional compressive strength, ease of production and maintenance, raw material availability, and cost-effectiveness [1,2]. When supplemented with admixtures, fibers, or alternative materials, concrete can achieve enhanced properties, contributing to superior final outcomes [3-7]. Composite concrete, often referred to as fiber concrete, involves reinforcing concrete through the addition of fibers to the mixture. This reinforcement bolsters strength, crack resistance, and overall mechanical performance [8]. Commonly employed fibers such as polypropylene, glass, steel, among others, augment both tensile and compressive strength, acting as supplementary reinforcement to mitigate cracking and fortify concrete [9,10].

Fiber-reinforced composites have garnered significant attention in various industries due to their exceptional mechanical properties and versatility in applications. Among the myriad of fibers utilized in composite manufacturing, rattan fibers stand out for their unique characteristics and potential contributions to composite material properties [11]. However, understanding the effects of different fiber lengths, particularly rattan fibers, on

*Corresponding author: andiyusra@utu.ac.id

^a orcid.org/0000-0003-4779-0815; ^b orcid.org/0009-0004-5007-9906; ^c orcid.org/0009-0001-9153-3712;

^d orcid.org/0009-0001-1959-8677; ^e orcid.org/0000-0003-1807-1088

DOI: <http://dx.doi.org/10.17515/resm2024.208me0305rs>

Res. Eng. Struct. Mat. Vol. x Iss. x (xxxx) xx-xx

the structural and chemical properties of composites requires comprehensive investigation.

Effect of Fiber Length on FTIR Analysis. Fourier Transform Infrared Spectroscopy (FTIR) serves as a powerful tool for analyzing the chemical composition and molecular structure of materials [12]. Literature studies suggest that varying fiber lengths can influence the FTIR spectra of composite materials [13]. Rattan fibers, with their distinct chemical composition and arrangement, may exhibit nuanced spectral signatures that elucidate their role in composite structures [14].

Impact on Macro and Microstructure. Macro and microstructural characteristics play pivotal roles in determining the mechanical behavior and performance of composite materials [15]. The arrangement and alignment of fibers, influenced by their length, significantly impacts structural integrity and overall properties. Investigations into the macro and microstructure provide insights into the interfacial interactions between fibers and matrix, thereby facilitating the optimization of composite design and fabrication processes [16].

Despite the evident significance of studying the effects of fiber length, particularly rattan fibers, on FTIR analysis, macro, and microstructure, a comprehensive examination remains scarce in the existing literature. This knowledge gap underscores the need for further research to elucidate the intricate relationships between fiber characteristics and composite properties, thereby unlocking the full potential of rattan fibers in composite applications [17]. Fiber concrete exhibits notable resistance to cracking, attributed to the control of small cracks induced by factors like drying, temperature fluctuations, or structural loads [18]. Its application is prevalent in earthquake-resistant construction, as fibers mitigate vibrations, averting severe structural damage during seismic events [19]. Certain fiber types, like polypropylene, offer increased strength without a significant weight increase, facilitating material transportation and manipulation [20]. Moreover, fibers such as glass or polymer variants provide corrosion resistance, enhancing durability in aggressive environments [21].

The utilization of composite concrete offers extensive design flexibility, permitting intricate architectural designs [22]. Indonesia, endowed with extensive forest resources covering over half of its territory, notably produces rattan, prized for its lightweight nature and exceptional tensile strength, [23]. Incorporating rattan into concrete holds promise for enhancing flexibility and durability in both compressive and tensile strength. Rattan fiber, commonly integrated into concrete mixtures, is recognized as 'micro reinforced concrete' or 'fiber concrete' (FC) [24]. The inclusion of rattan fiber reinforces concrete, reducing cracks induced by shrinkage or temperature changes and enhancing resistance to environmental and chemical pollutants [25]. Furthermore, rattan fibers improve concrete's tensile strength, elasticity, and resistance to vibrations and earthquakes, thereby preventing structural damage. They also increase bending strength, rendering concrete more resilient to loads and deformations while reducing overall structure weight, consequently conserving energy during construction and transportation processes [26,27].

The length of fibers significantly influences concrete's performance, impacting aspects like tensile strength, crack resistance, and durability. Short fibers are adept at controlling micro-cracking, while long fibers span larger cracks, collectively enhancing concrete's durability against dynamic loads [28]. Scanning Electron Microscope (SEM) and Energy Dispersive X-ray Spectroscopy (EDS) analyses offer insights into fiber distribution, chemical composition, and interaction with concrete matrices, aiding in evaluating mechanical performance and guiding concrete formulation improvements [29-33]. Additionally, Fourier Transform Infrared Spectroscopy (FTIR) facilitates the identification

of concrete components, quality assessment, and pollution monitoring, crucial for optimizing composite concrete performance [34]. By varying fiber lengths, the study aims to enhance mechanical properties, targeting increased strength, ductility, and crack resistance, aligning with engineering specifications for superior structural performance [35].

In the study, we will explore the influence of fiber length variations, particularly rattan fibers, on various structural aspects of concrete, including FTIR (Fourier Transform Infrared Spectroscopy) analysis, macrostructure, and microstructure. Rattan fibers have become an attractive additive in concrete, but the influence of fiber length on the mechanical properties and structure of concrete is still not fully understood. By combining FTIR techniques with macro- and microstructural analysis, this study aims to provide in-depth insights into how rattan fiber length affects the chemical and physical characteristics of concrete, as well as how it relates to its mechanical performance. One of the novelties offered by this article compared to previous ones is the focus on the influence of variations in rattan fiber length on the behavior of concrete microstructure. The article not only covers the characterization of the mechanical properties of concrete with fiber additions but also examines how the distribution of fibers within the concrete matrix and the overall structure change with varying fiber lengths. This provides a deeper understanding of how the micro composition of concrete reacts to changes in fiber length.

The novelty discovered in this study lies in the observation of maximum compressive strength in concrete mixes utilizing a fiber length of 30 mm. Typically, prior research has shown that the highest compressive strength was achieved when fibers with lengths ranging from 2 to 2.5 mm were used, as documented by [36]. Additionally, this study presents a novel finding regarding the emergence of compound functional groups, with distinctions between non-fiber concrete and rattan fiber concrete. The incorporation of clam shell ash at a 4% dosage resulted in a significant enhancement of compressive strength. Despite the relatively low cement content in the samples, a substantial increase in compressive strength was achieved through the combination of 30 mm rattan fibers and a 4% addition of clam shell ash.

2. Materials and Testing Method

2.1. Materials

Materials used to make normal-quality concrete include Portland Cement Composite (PCC), coarse aggregate (natural stone), fine aggregate (sand), shell powder, rattan fiber, and water. The cement chosen for this study is PCC cement. Laboratory examination of this cement will not be carried out because it adheres to standards. Visual inspection will only be done on the cement bag to ensure there is no damage such as tears and no hard lumps present. Portland cement composite is a mixture of materials consisting of Portland cement and other additives such as fillers, additives, or fibers to improve the performance of concrete.

The Chemical and Physical Properties of Portland Cement Composite are as follows. One of the main properties of Portland cement is its ability to react with water, forming strong hydration. This hydration process produces products such as calcium silicate hydrate (CSH) and calcium hydroxide (CH), which give strength and hardness to concrete. The chemical composition of Portland cement is mainly composed of cement clinker, which contains tricalcium silicate (C_3S), dicalcium silicate (C_2S), tricalcium aluminate (C_3A), and tetra calcium alumina ferrite (C_4AF). The relative proportions of each of these minerals can affect the performance and properties of the resulting concrete. Portland cement composites generally contain silica, which plays an important role in forming CSH during the hydration process. Silica can also increase concrete's resistance to corrosion and

chemical attack. Portland cement composite also contains an additive, pozzolan. In the past, PCC was known as Portland Pozzolan Cement (PPC); this type of cement is also referred to as Type II cement [37].

Portland cement has a relatively high density, ranging from 3.10 to 3.25 g/cm³, depending on the composition and manufacturing process. Portland cement composite exhibits a hardness that is not excessively high when compared to Type I cement or Portland Cement (PC) after the hydration process is complete, yet it provides the mechanical strength necessary for construction applications. The optimum hardness period of PCC cement (Type II cement) is slower compared to PC cement (Type I cement). Concrete made from Portland cement composite tends to have varying porosity, depending on the composition of the mixture and the casting method [38]. This porosity can affect the physical and chemical properties of concrete, such as resistance to chemical attack and water permeability.

Clam shell ash, a common additive in concrete production, has varied physical and chemical traits. It typically presents as fine powder with diverse particle sizes based on production methods. Its low density facilitates even distribution within concrete mixtures. The ash's porous nature enhances concrete permeability and moisture absorption. Rich in calcium carbonate, derived from shellfish, it may contain other minerals. Its reactive properties influence cement hydration, fostering additional hydration products for concrete enhancement. The ash's calcium carbonate content can elevate concrete pH, impacting its chemical behavior. Table 1 details clam shell ash's chemical composition.

Table 1. Chemical composition of CSA [39]

Oxides	SiO ₂	Al ₂ O ₃	Fe ₂ O ₃	CaO	MgO	SO ₃	K ₂ O	Na ₂ O	P ₂ O ₅	Cl	Sr	LOI
CSA (%)	6.95	2.59	2.40	81.60	3.07	1.20	0.30	0.00	0.55	0.20	0.50	0.77

Coarse aggregates derived from natural stone and fine aggregates derived from sand will be sourced from the KRUENG Nagan River, Nagan Raya Regency. Inspection of coarse aggregate (natural stone) and fine aggregate (sand) as raw materials for concrete requires an examination of physical properties to meet planned standards. This examination includes aggregate properties such as specific gravity, absorption, bulk density, and sieve analysis.

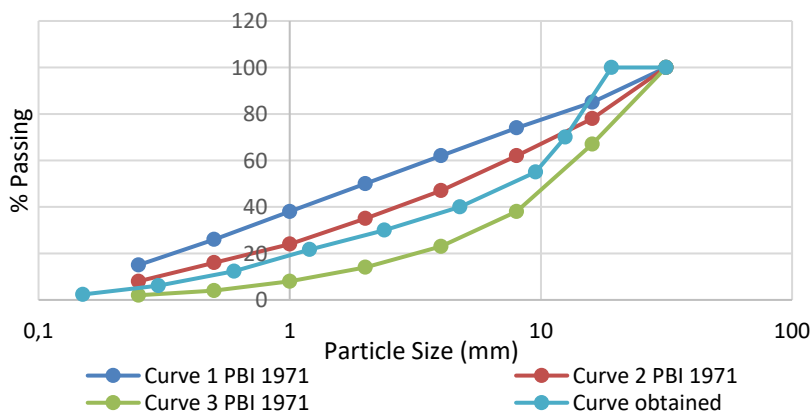


Fig. 1. Particle size distribution of aggregates

The shells used will be obtained from UJONG BAROH Village, Johan PAHLAWAN District, West Aceh Regency. The next step involves cleaning and drying the shells, after which they will be crushed until they reach a powder form with a size that can pass through sieve number 200. Figure 1 shows the granular gradient used in this study. The rattan fiber to be used will be sourced from the SIEMEULUE Regency area. After obtaining the rattan, the material will undergo a drying process to reduce water content. Next, the rattan will be cut into short segments and then split to obtain fiber strands with a thickness of about ± 1 mm. Afterward, the fibers will be cut to the planned lengths of 20 mm, 30 mm, and 40 mm. Figure 1 shows the rattan fiber material used in this study. The length of rattan fiber mixed into fresh concrete has different lengths, namely 20 mm, 30mm and 40 mm with an average diameter of 1 - 2 mm.



Fig. 2. (a) Rattan fiber, (b) clam shell ash

Shell ash is a solid remnant resulting from the burning of clam shells. The chemical properties of clam shell ash may vary depending on the type of shellfish used and the combustion process applied. Here are some common chemical properties of clam shell ash: Mineral Content: Shell ash generally contains minerals such as calcium carbonate (CaCO_3) which is the main component of clam shells. In addition, shell ash can also contain small amounts of other minerals such as silica (SiO_2), alumina (Al_2O_3), and iron oxide (Fe_2O_3). Calcium oxide (CaO) is the main component produced from the burning of calcium carbonate in the shell of the shell. The CaO content in the shell ash of the shells can contribute to the hydraulic binding properties in the concrete mixture. Silica Content, some types of shell ash also contain silica (SiO_2), which is a common component in pozzolanic materials. Silica in the ash of clam shells can provide pozzolanic reactivity, which can increase the strength of concrete. The chemical properties of shell ash are also affected by the carbonate content that remains in the shell of the shell that has not yet fully burned. This residual carbonate can affect the chemical properties and reactivity of shell ash shells in the concrete mixture. Heavy Metal Content although in small amounts, clamshell ash can also contain heavy metals such as lead (Pb), cadmium (Cd), and mercury (Hg) that can affect the environment and human health if not managed properly. An understanding of the chemical properties of shellfish ash is important in its use as an additive in concrete mixtures. By understanding the chemical composition of clam shell ash, engineers can design optimal concrete mixtures by improving the performance and durability of concrete and minimizing negative impacts on the environment and human health.

In the study, to obtain the gradation value of the aggregate, it was obtained from sieve analysis data which was carried out by filtering the aggregate using a set sieve / sieve. Data obtained from sieve analysis is used to see the granular arrangement of aggregates used in concrete mixtures. The results of the calculation of sieve analysis and Fineness Modulus can be seen in Table 2.

Table 2. The value of the modulus fineness (FM) of the aggregate.

No.	Type of Aggregates	Modulus Fineness	Reference
		FM (%)	ASTM
1	Coarse Aggregate (8-12 mm)	5.983	5.5 - 8.5
2	Fine Sand (0-2 mm)	3.1	2.2 - 3.1

From Table 2, the calculation of the value of Fineness Modulus against coarse aggregate is 5.983%. The Fineness Modulus value of coarse aggregate (coarse aggregate) meets ASTM requirements, which ranges from 5.5 - 8.5%. While the calculation of the Fineness Modulus value for fine sand, which is 3.1%, has met ASTM [26] requirements, which ranges from 2.2 - 3.1%.

2.2. Mix Design

This research will use a concrete mixture with a plan quality of 20 MPa. The concrete mix planning method refers to the method issued by the American Concrete Institute, [40]. The standard specimen to be used is cylindrical with a diameter of 15 cm and a height of 30 cm, with a maximum aggregate diameter of 19 mm. The planning process for a 20 MPa concrete mix starts with determining the slump test value, followed by calculating water quantity based on slump test and maximum aggregate. Then, the Cement Water Factor (w/c) is determined for concrete quality. Cement weight is found by subtracting pre-calculated water amount from w/c. Coarse aggregate amount is calculated based on maximum aggregate diameter and fine aggregate's fineness modulus. Fine aggregate quantity is determined from total concrete weight minus water, cement, and coarse aggregate. The study focuses on comparing concrete non fiber (CNF) with concrete containing rattan fiber (RF) of 20 mm, 30 mm, and 40 mm lengths, each at 0.5% fiber ratio, and 4% clam shell ash added to cement weight.

Table 3. Material composition for each test specimen variation

No	Material	24 Specimens				Total	Unit
		CNF	RF 20 mm	RF 30 mm	RF 40 mm		
1	Cement	14.9	14.9	14.9	14.9	59.7	Kg
2	Water	7.7	7.7	7.7	7.7	30.966	Kg
3	Coarse Aggregate	41.4	41.4	41.4	41.4	165.8	Kg
4	Fine Aggregate	26.2	26.2	26.2	26.2	105.1	Kg
5	Clam Shell Ash (4%)	0.0	0.6	0.6	0.6	1.8	Kg
6	Rattan Fibre (0,5%)	0.0	75.0	75.0	75.0	225.0	gr

The implementation of this research will be made a total of 24 test objects with a cylindrical shape (Ø 15 cm, T = 30 cm), the test specimens will be carried out by

distinguishing the length of rattan fiber as an added material, namely concrete without fiber, fiber concrete 20 mm, fiber concrete 30 mm, and fiber concrete 40 mm. The mix design is for 24 test specimens, there are 4 specimen's variations, namely CNF, CRF 20mm, CRF 30mm and CRF 40 mm, each variant is made with 3 tests for compressive tests and 3 pieces for concrete split tensile strength, the total number of test objects is all 24 pieces.

2.3. Compressive Strength

The concrete compressive strength testing scheme (concrete cylinder), and to carry out concrete compressive strength testing will follow several stages as follows. The specimen will be placed on the press centrally in a vertical position. The press will be run with constant load additions ranging from 2 to 4 kg/cm² per second; Loading will be carried out until the specimen is destroyed, and the maximum load that occurs during the specimen inspection is recorded, [44,45].

2.4. Scanning Electron Microscope-EDS (SEM-EDS)

SEM testing, among other techniques, can be utilized to ascertain information about surface properties, particle shape and size, as well as particle distribution and arrangement. Our scanning electron microscope (SEM) equipped with energy-dispersive X-ray spectroscopy (EDS) (ZEISS EVOMA10) facilitates such testing [41]. SEM-EDS (Scanning Electron Microscope-Energy Dispersive X-ray Spectroscopy) is a test equipment used to test material samples, including composite concrete samples.

Here are some of the uses of the SEM-EDS test equipment in testing composite concrete samples. Surface Morphology Analysis: SEM offers high-resolution views of composite concrete surface structures, aiding in crack, porosity, and phase distribution identification. Integrated with SEM, EDS enables chemical element identification and mapping on sample surfaces, facilitating the understanding of chemical element distribution and phase distribution. EDS permits the chemical composition analysis of composite concrete samples, ensuring material quality and performance. SEM-EDS aids in identifying material phases in composite concrete samples, enhancing understanding of material microstructure and properties. Thus, SEM-EDS significantly contributes to the characterization of composite concrete, enhancing understanding of its structure, composition, and properties, [1,8,9, 10,18,29,30,42]

2.5. FTIR

FT-IR is used to determine functional groups in materials through the study of molecular interactions, which are demonstrated by the transmission of infrared light in various forms. This study focuses on the effect of treatment on the functional groups of composite concrete and fibers, as well as differences in the expression of functional groups in conventional concrete, [31-33]. The specimens used in the Fourier Transform Infrared Spectroscopy (FTIR) test will be taken from cylindrical specimens with additional variations of rattan fiber and shell powder that have been used in compressive strength and tensile strength tests, in the form of small flakes. The application of FTIR Analysis for fiber concrete testing involves sample preparation with KBr pellet making. The sample is refined with mortar to homogenize it. A small amount of sample is then placed into the barn, and KBr powder is added in a ratio of 1:10. The sample and KBr powder are ground until homogeneous, after which the mixture is inserted into the KBr pellet dies. The KBr pellet dies are then closed and pressed using a mini-Press KBr pellet. The formed KBr pellet is inserted into the sample holder in the FTIR. The FTIR test scheme can be seen in Figure 3., and to carry out the FTIR test, several stages must be followed as follows: Concrete samples are cleaned from contaminants or dust that may affect test results. The FTIR Spectrometer is turned on, and the system is allowed to reach stable operating conditions, ensuring that all optical components and instrument detectors are in good condition. The

concrete sample is placed on the IR (infrared) glass, ensuring that it is flat on the IR glass to produce accurate test results. FTIR spectrum measurements are then performed by directing infrared light onto the concrete sample. After the measurement is complete, the FTIR analysis software will identify the chemicals and main components in the concrete sample.

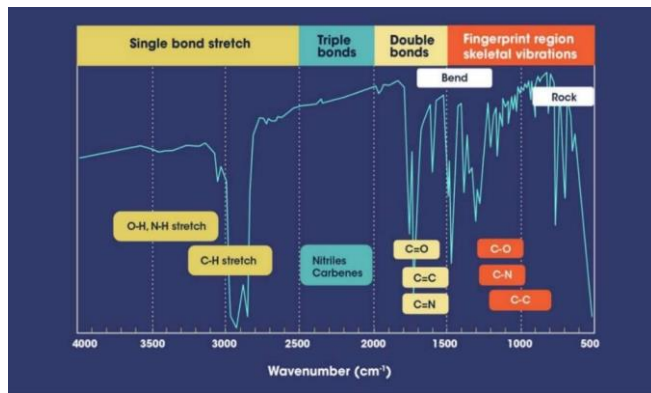


Fig. 3. Infrared absorption area, [34]

3. Results and Discussion

3.1 Sump test

In normal concrete, slump testing is carried out which aims to determine the viscosity of the concrete mixture. This factor is due to the addition of fiber to the concrete mixture.

The data obtained from the results of the slump test in each casting of each fiber variation are shown in Figure 2. From these data, the value of the concrete mortar slump ranges from 7.5 cm – 10 cm, which means that it is in accordance with the height of the planned slump.

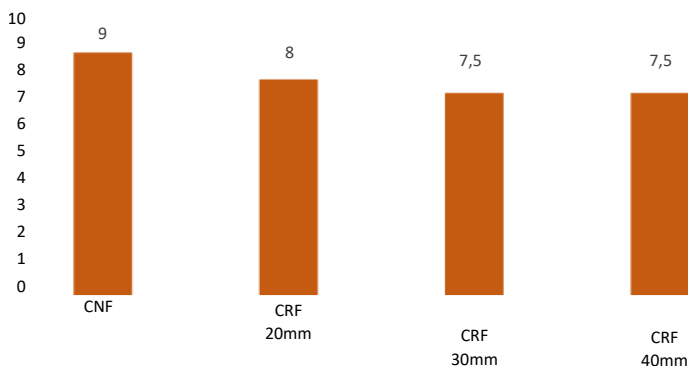


Fig. 4. Slump test results graph

Fig. 4 shows that the shape of the slump has a difference. In this study, the resulting high slump test showed that the value of the slump value was influenced by the percentage of fiber mixed into the concrete mortar. The graph below shows that the lowest slump values are in 30 mm and 40 mm 2 rattan fibers, while in normal concrete without the addition of rattan fibers and shell ash produces the highest slump values of 9 cm. This shows that the higher the length of rattan fiber used, the higher the water absorption of concrete.

3.2 Strength of Concrete

After the specimen is removed from the soaking bath following the treatment process, tests can be performed as shown in Fig. 5. Then, the specimen is left for 24 hours until it reaches a surface dry state. After that, the specimens are weighed to determine the weight per specimen. Next, compressive strength testing is performed on the test specimen using a pressure testing machine. Normal concrete compressive strength testing is carried out according to the planned life, which is 28 days concrete life. Data on concrete compressive strength test results at 28 days of age, compressive strength graphs can be seen in Figure 4.

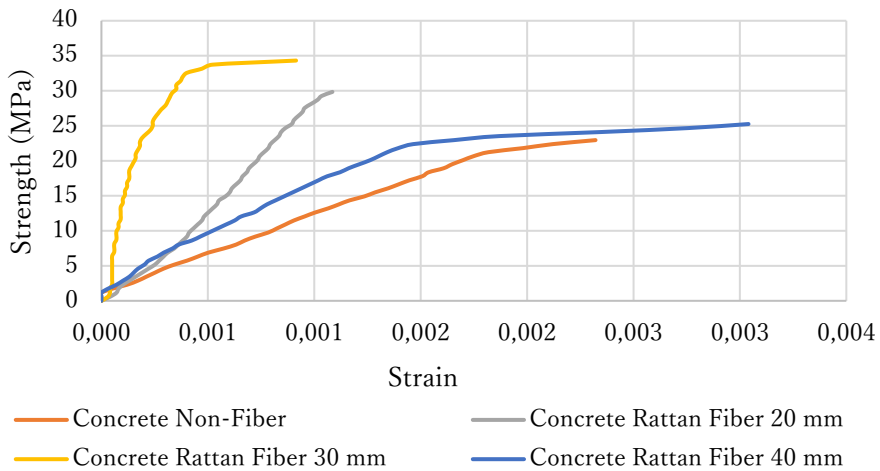


Fig. 6. Stress-strain relationship of rattan fiber concrete with variations in fiber length

Based on Figure 6, it can be observed that composite concrete using a 40 mm fiber length exhibits greater deformation compared to both non-fiber concrete and fiber concrete variations with 20mm and 30mm fiber lengths. This indicates that fiber concrete with a length of 40mm displays more ductility compared to fiber concrete with shorter fiber lengths, despite the compressive strength of the former being 40mm lower than that of the latter. According to Figure 6, the obtained compressive strengths are as follows: CNF 22.120MPa, CRF 20mm 23.488MPa, CRF 30mm 31.011MPa, and CRF 40mm 19.085MPa. This suggests that the optimum strength of fiber concrete is achieved with a 30mm CRF fiber length.

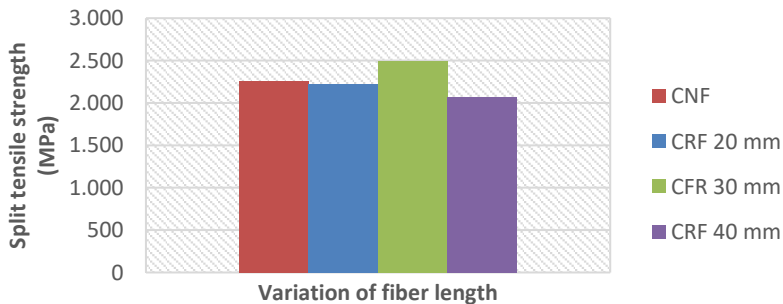


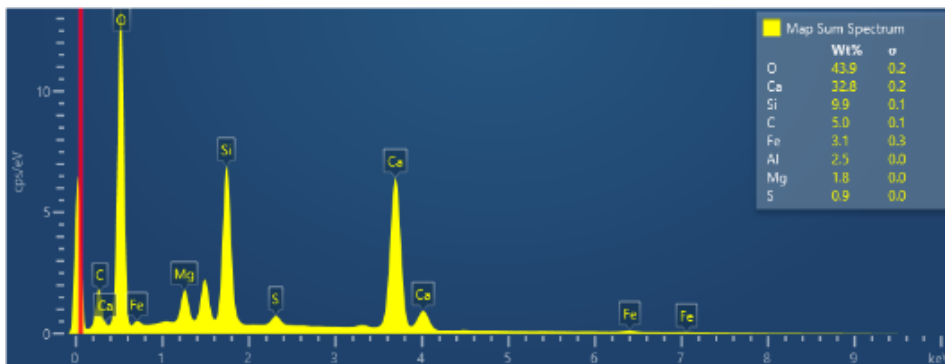
Fig. 7. Split tensile strength of CRF with variations in fiber length

In Fig. 7 above, the results of tensile strength tests conducted on fiber concrete at the age of 28 days are presented. Tensile strength is a measure obtained by breaking a concrete cylinder into two parts with a force applied perpendicular to its long axis. The tensile strength of each specimen is measured in units of N/mm^2 . Additionally, there is a column showing the increase in tensile strength from one specimen type to another, calculated in units of N/mm^2 and as a percentage. Here is a discussion of the tensile strength data provided. CNF (Concrete Non-Fiber), Tensile strength $2.265N/mm^2$. No change in strength compared to CNF (0%). CRF 20 mm (Concrete with 20 mm rattan Fiber), Tensile strength $2.218 N/mm^2$. Decrease of -2.1% compared to CNF. CRF 30 mm (Concrete with 30 mm Steel Fiber), Tensile strength $2.501N/mm^2$. Increase of 9.4% compared to CNF. CRF 40 mm (Concrete with 40 mm Steel Fiber): Tensile strength $2.076N/mm^2$. Decrease of -9.1% compared to CNF. Conclusion: Adding steel fibers to concrete can increase or decrease tensile strength depending on fiber length and material characteristics. 30 mm steel fibers significantly increase tensile strength, while longer or shorter fibers do not yield similar results. From the discussion above, it can be concluded that the addition of steel fibers in concrete can increase or even reduce tensile strength depending on the length of the fibers and their material characteristics. In these cases, the addition of 30 mm steel fibers results in a significant increase in tensile strength, while longer or shorter fiber lengths do not yield equally good results.

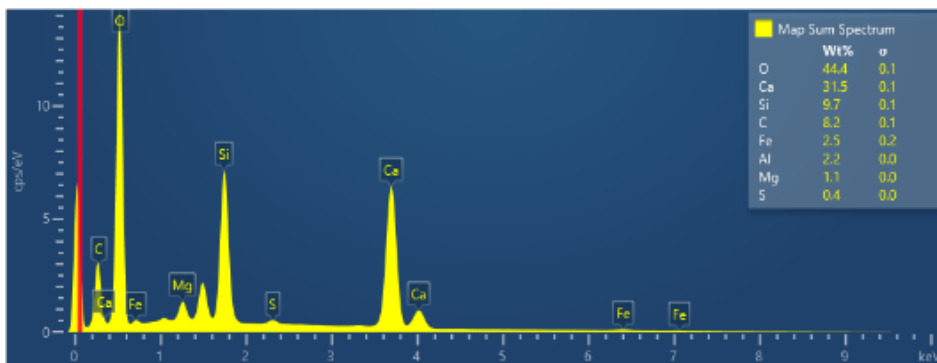
3.3 SEM-EDS Analysis

The findings of the study suggest that incorporating rattan fibers into concrete can result in either an increase or decrease in tensile strength, depending on the fiber length and material characteristics. Specifically, the inclusion of 30 mm rattan fibers notably enhances tensile strength, while longer or shorter fiber lengths do not produce similarly favorable outcomes. Furthermore, chemical composition analysis of the concrete reveal’s variations upon the addition of rattan fibers, indicating changes in elemental composition. Morphological observations conducted using Scanning Electron Microscopy (SEM) offer detailed insights into the microscopic structure of concrete surfaces, both with and without fibers.

Fig. 8.a shows the results of the chemical composition of sample (a) non-fiber concrete. The data provided has the weight percentage (Wt.%) of the various elements in the sample. Where describe the result as follows. Chemical analysis shows that Oxygen (O) has a weight percentage of 43.9%, Calcium (Ca) is 32.8%, Silicon (Si) has two entries, namely 9.9% and 0.9%, Carbon (C) is 5.0%, Iron (Fe) is 3.1%, Aluminum (Al) is 2.5%, and Magnesium (Mg) is 1.8%. This chemical composition indicates that Oxygen, Calcium, and Silicon are the most dominant elements in non-fiber concrete samples.



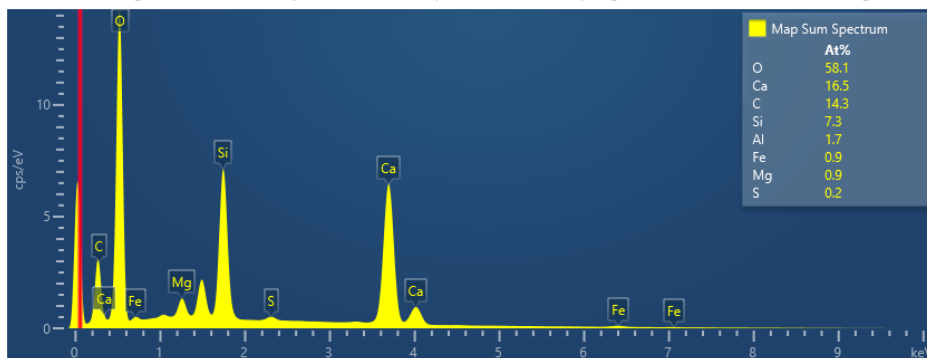
(a) Non-Fiber concrete



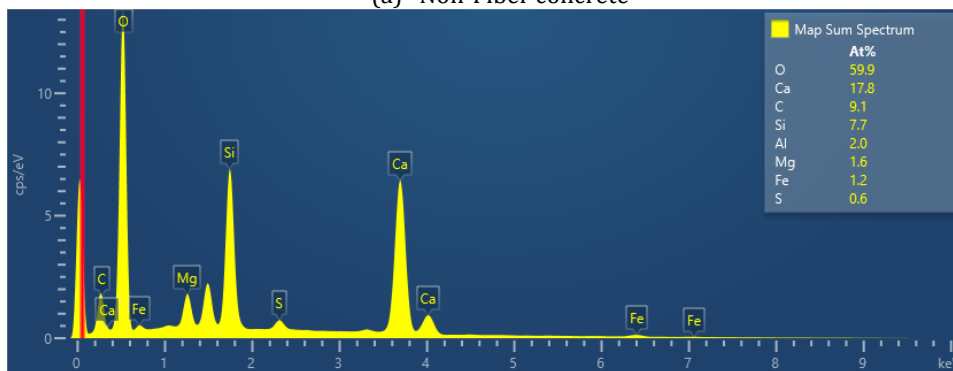
(b) Fiber concrete

Fig. 8. SEM-EDS test results of concrete base the weight percentage (Wt.%)

Figure 8.b illustrates the distribution of chemical elements in a concrete specimen with rattan fibers, shown in weight percentages. Oxygen dominates at 43.9%, followed by Calcium at 32.8%, Silicon at 9.9%, Carbon at 5.0%, Iron at 3.1%, Aluminum at 2.5%, Magnesium at 1.8%, and Sulphur at 0.9%. These proportions suggest the presence of oxide, calcium-rich, silicate, organic, iron-containing, aluminum-rich, magnesium-containing, and Sulphur-containing compounds, respectively. This data provides insight into the sample's chemical composition, aiding further analysis to identify specific minerals or compounds.



(a) Non-Fiber concrete

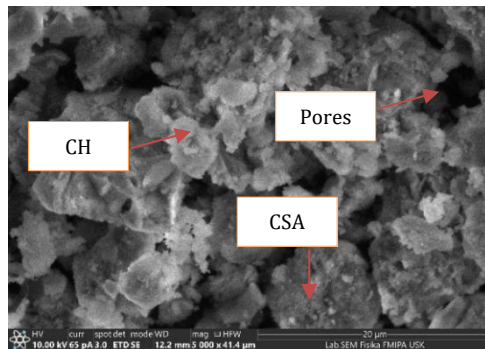


(b) Fiber concrete

Fig. 9. SEM-EDS test results of non-fiber concrete (At%).

Fig. 9.b visualizes the percentage composition of elements in a sample. Oxygen (O) dominates with 59.9%, followed by Calcium (Ca) at 17.8%, Carbon (C) at 9.1%, Silicon (Si)

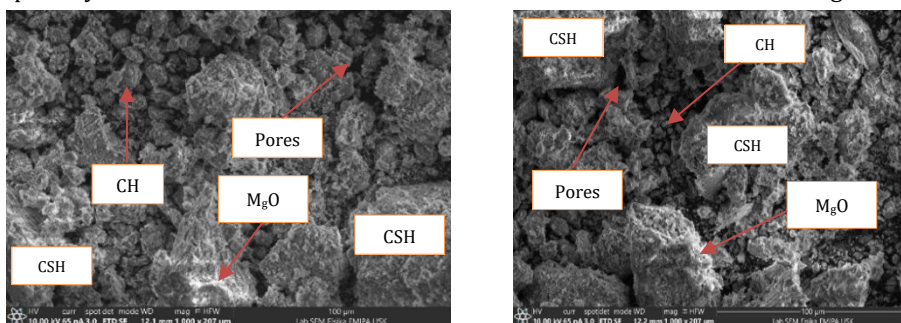
at 7.7%, Aluminum (Al) at 2.0%, Magnesium (Mg) at 1.6%, Iron (Fe) at 1.2%, and Sulphur (S) at 0.6%. The diagram shows the relative proportions of each element with sectors proportional to their percentage composition. Figure 9.b depicts composition Map spectra, showing the relative proportions of chemical elements in a sample. Data highlights the percentages of elements: Oxygen (O): 43.9%, Calcium (Ca): 32.8%, Silicon (Si): 9.9%, Carbon (C): 5.0%, Iron (Fe): 3.1%, Aluminum (Al): 2.5%, Magnesium (Mg): 1.8%, Sulphur (S): 0.9%. These visuals provide insight into element distribution, with Oxygen (O) being the highest, followed by Calcium (Ca), and so on. Figure 10 shows the difference between CNF concrete and fiber concrete with the addition of clam shell ash (CSA), the amount of element C (Carbon) is higher in concrete with the addition of CSA. In Figure 9, fiber concrete has a higher oxygen and carbon value compared to non-fiber concrete.



Fiber concrete

Fig. 10. Micromorphological form of concrete by SEM

Fig. 10 shows the hydration results of cement. There are MgO , CSA, CH, and micropores measuring 5 microns. The fiber concrete microstructure with quite a lot of pores marked in black in the figure. There is a matrix shape of cement and CSA and sand, but the number of white fibers is not too visible. Calcium Silicate Hydrate (CSH), This compound is formed during the hydration process of Portland cement, which is the main component of concrete. CSH provides strength and durability to concrete. Also formed during hydration of Portland cement, CH is a byproduct of chemical reactions and contributes to the performance of concrete. Magnesium Oxide (MgO), Also present in some composite concrete mixtures, MgO can affect the chemical and physical properties of concrete, especially in the context of resistance to chemical attack and mechanical strength.



(a) Non-Fiber concrete

(b) Fiber concrete

Fig. 11. Micromorphological form of CNF structure (a), CRF (b)

Fig. 11.a shows CH compounds that occur due to imperfect cement hydration process. Fig. 10 and 11 shows SEM analysis revealing the surface structure of concrete materials on a microscopic scale. With high resolution, SEM scanning enables detailed observation of

surface structures such as pores, cracks, and aggregates, providing important insights into the quality and strength of concrete. The microstructure of non-fiber concrete, including pore size, can be observed. Pore size and particle size in non-fiber concrete are visible through SEM analysis within the range of 20 microns. Morphological differences between non-fiber concrete and fiber concrete, especially with the addition of shell ash, are evident. In Figure 11, rattan fibers are shown attached to the concrete matrix, contributing to strong tensile strength in concrete. Concrete with rattan fiber exhibits greater tensile strength compared to other concrete variations. In Figures 11.a and 11.b, shows the difference in crystal shape between non-fiber concrete and fiber concrete. In fiber concrete with added shell ash, the distance between particles is smaller compared to non-fiber concrete. The denser condition of fiber concrete to which shell ash is added is visibly apparent on the surface than in the SEM Image. Figure 11 depict Morphological Analysis at magnifications of 1000, and Fig. 10 5000 times, respectively. SEM analysis unveils the surface structure conditions of concrete materials on a microscopic scale. With high resolution, SEM scanning facilitates detailed observations of surface structures such as pores, cracks, and aggregates, offering crucial insights into the quality and strength of concrete. Microscopic conditions of non-fiber concrete structures, including the cement paste matrix and cement-sand matrix, can be observed. Pore sizes and elements in non-fiber concrete become visible through SEM analysis in the 100-micron range. In Figure 9.a, many small grains seem to separate from each other, possibly due to the addition of shell ash in concrete, as indicated in Figure 9.b. The SEM analysis in Figure 8.b reveals the surface characteristics of the fiber concrete material at the microscopic level, including pore size. SEM analysis can detect pore and particle sizes in non-fiber concrete up to 20 microns. In the figure, smaller pores are visible compared to non-fiber concrete, suggesting that fiber material may be filling these pores in concrete.

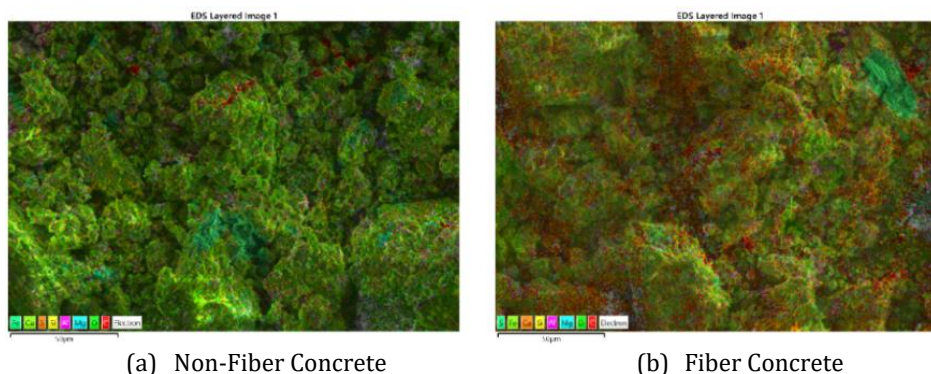


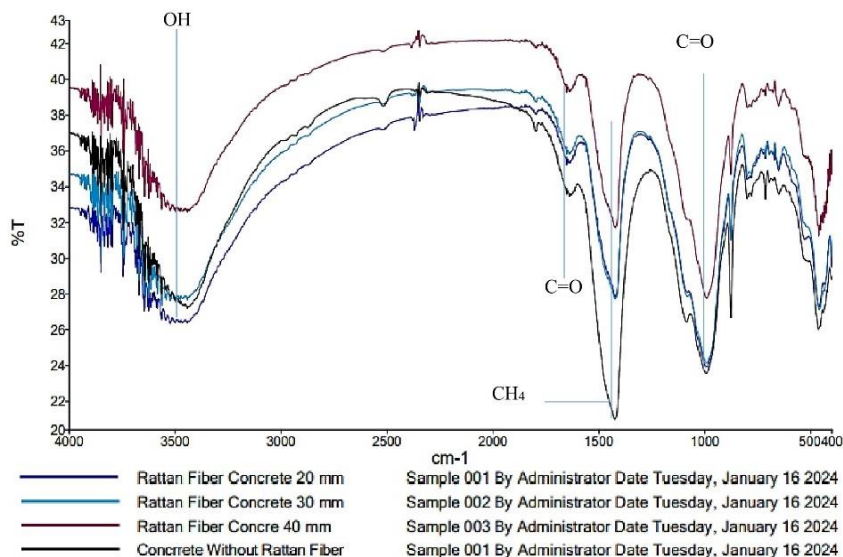
Fig. 12. The form of distribution of chemical elements in concrete

Based on Fig.9, and Figure 12.a, the chemical elements in non-fiber concrete are dispersed as follows: Oxygen (O): 59.9%, mainly found in oxide compounds like Calcium Oxide and SiO₂. Calcium (Ca): 17.8%, associated with compounds like calcium silicate and calcium hydroxide. Carbon (C): 9.1%, typically in carbonate or organic form. Silicon (Si): 7.7%, mainly in silicate compounds like SiO₂. Aluminum (Al): 2.0%, found in compounds like aluminum oxide. Magnesium (Mg): 1.6%, present in various minerals in aggregates. Iron (Fe): 1.2%, derived from compounds like iron oxide. Sulphur (S): 0.6%, likely in sulphate form. Figure 12 shows the distribution of chemical elements in non-fiber concrete visually, while Figures 12.a and 12.b provide further details. Additionally, in Figure 6.b, representing fiber concrete with clam shell ash, Carbon (C) distribution surpasses that of non-fiber concrete. Figure 4.b illustrates the spectra of composition maps, indicating the proportions of chemical elements within a given sample. The data showcases the percentages of elements as follows: Oxygen (O) constitutes 43.9%, Calcium (Ca) comprises

32.8%, Silicon (Si) accounts for 9.9%, Carbon (C) represents 5.0%, Iron (Fe) constitutes 3.1%, Aluminum (Al) contributes 2.5%, Magnesium (Mg) makes up 1.8%, and Sulphur (S) is at 0.9%. These visuals offer insights into the distribution of elements, with Oxygen (O) being the most abundant, followed by Calcium (Ca), and so forth.

3.4 FTIR Result

Based on Fig. 13 and Table 3, FTIR data from various types of concrete with and without rattan fiber, differences in absorption patterns indicate variations in the type and concentration of compounds present in the concrete. For instance, in concrete containing 20 mm rattan fiber, an absorption peak at 3.525.54 cm^{-1} suggests the stretching of O-H bonds, typically associated with the presence of carboxylic acids. Conversely, in concrete without rattan fibers, an absorption peak at 3.590.86 cm^{-1} indicates the presence of O-H stretch bonds, potentially suggesting the existence of phenols or alcohols.



Sample Name	Description	Quality Checks
Rattan Fiber Concrete 20 mm – 40 mm & Concrete Without Rattan Fiber	By Administrator Date Tuesday, January 16 2024	The Quality Checks give rise to multiple warnings for the sample.

Fig. 13. Compound groups in concrete

Table 4. Test results of functional groups of rattan fiber concrete compounds

Concentrate (%)	Absorption Area (cm^{-1})	Compound Type	Bounds And Types of Functional Group	Intensity
CRF 20 mm	3,525.54	carboxylic acid monomer	O-H Stretching	Medium
	1,651.00	Alkene	C=O Stretching	Capricious
	1,420.00	Alkane	CH ₄ Bending	Strong
	894.38	Alkene	C=O Stretching	Strong
CRF 30 mm	3,590.91	phenol, alcohol monomer	O-H Stretching	Capricious
	3,500.08	carboxylic acid monomer	O-H Stretching	Medium

	1,638.24	Alkene	C=O Stretching	Capricious
	1,420.12	Alkane	CH ₄ Bending	Strong
	988.35	Alkene	C=O Stretching	Strong
CRF 40 mm	3,564.10	hydrogen bond alcohol, phenol	O-H Stretching	Capricious
	1,650.97	Alkene	C=O Stretching	Capricious
	1,420.12	Alkane	CH ₄ Bending	Strong
	989.03	Alkene	C=O Stretching	Strong
CNF	3,590.86	hydrogen bond alcohol, phenol	O-H Stretching	Capricious
	1,637.55	Alkene	C=O Stretching	Capricious
	1,424.42	Alkane	CH ₄ Bending	Strong
	992.07	Alkene	C=O Stretching	Strong

Based on Table 4, it can be inferred that 30mm CRF fiber concrete exhibits stronger compressive strength compared to normal concrete, as it possesses 5 bond compounds as opposed to CNF fiber concrete, which only has 4 bonding compounds. Similarly, other variations of fiber concrete exhibit only 4 compound bonds. Regarding the condition of 40 mm CRF concrete, it is anticipated to have lower compressive strength than other concrete variations due to the excessive length of the fiber, resulting in many areas of concrete being filled with fiber beyond the standard 20mm fiber length, leading to reduced compressive strength. However, it boasts advantages in tensile strength with greater deformation than other concrete variations. For a more comprehensive study, the author plans to continue the research by conducting tests on the pure bending strength of fiber concrete. The data are interpreted in Figure 13 and Table 4, all based on the guidelines in Figure 3 Infrared absorption area [34].

4. Conclusions

This study presents significant findings regarding the effect of rattan fiber length variations on the mechanical properties, characterization, and microstructure of concrete. Based on the test results and discussions that have been presented, several conclusions can be drawn to provide a deeper understanding of this topic.

- First, from the results of the slump test, the addition of rattan fiber to concrete affects the slump value, where the highest slump value occurs in normal concrete without the addition of rattan fiber, while the lowest slump value occurs in concrete with the addition of 30 mm and 40 mm rattan fibers. This shows that the longer the rattan fiber used, the higher the water absorption by concrete.
- Furthermore, from the results of the compressive strength test, it was found that concrete with a fiber length of 30 mm has optimal compressive strength compared to other concrete. Despite having lower compressive strength than fibreless concrete, concrete with a fiber length of 30 mm shows a significant increase in compressive strength compared to concrete with a longer or shorter fiber length.
- Later, in terms of tensile strength, it was found that the addition of steel fibers to concrete can increase or decrease tensile strength depending on the length of the fibers and material characteristics. Steel fibers with a length of 30 mm significantly increase the tensile strength of concrete, while fibers with longer or shorter lengths do not give the same results.
- In terms of chemical characterization, composition analysis shows that the chemical composition of concrete changes with the addition of rattan fibers. Rattan fibers enrich concrete with elements such as oxygen, calcium, silicon, carbon, iron,

aluminum, magnesium, and sulfur, all of which affect the chemical properties and reactivity of concrete.

- In microstructural analysis using SEM, significant differences were found between concrete microstructures with and without rattan fibers. Rattan fibers fill the pores of concrete and improve aggregate distribution, which can affect the overall physical and mechanical properties of concrete.
- In addition, the results of FTIR analysis show that variations in the absorption patterns of the spectrum show differences in the types and concentrations of compounds present in concrete. This suggests that the addition of rattan fibers can also affect the overall chemical properties of concrete.

Based on the FTIR testing data presented, this scientific work highlights several novelties that can be a significant contribution to materials research. Here are some identifiable points of novelty:

- **Analysis of Differences in Absorption Patterns:** In the FTIR test, there are differences in absorption patterns between CRF (Concrete Rattan Fiber) fibers with lengths of 20 mm, 30 mm, and 40 mm, and CNF (Concrete non-fiber) fibers. This indicates that fiber length has a significant influence on the chemical properties of the resulting material. This diversity of absorption patterns indicates that each type of fiber has unique chemical characteristics.
- **Functional Group Identification:** FTIR data shows the presence of various functional groups detected in each type of fiber. For example, carboxylic acid monomer groups were detected in 20 mm and 30 mm CRF fibers, as well as hydrogen bond alcohol and phenol in 40 mm CRF and CNF. The determination of these functional groups provides further understanding of the chemical composition of the fibers used in this study.
- **Absorption Intensity:** The level of absorption intensity in each functional group can also provide additional insight into the quantity or concentration of each compound involved. For example, the intensity of the medium in the carboxylic acid monomer group on 20 mm CRF fibers indicates a significant concentration of these compounds in the material.
- **Comparison Between Fiber Types:** Through the analysis of FTIR data, this scientific work makes it possible to compare chemical responses between different types of fibers, such as CRF of different lengths and CNF. Differences in absorption patterns and functional groups detected between fiber types can provide valuable information about the potential uses of each fiber in specific material applications.

This research provides a deeper understanding of the effect of rattan fiber length on the mechanical properties, characterization, and microstructure of concrete. The results of this research have important implications for the development of more efficient and sustainable construction materials in the future. Therefore, for follow-up studies, it is recommended to continue the research considering aspects such as environmental durability, dimensional stability, and long-term performance of concrete with rattan fiber. Thus, greater progress can be achieved in the field of construction materials engineering.

Acknowledgement

First and foremost, we extend our deepest appreciation to our supervisor, Prof. Ishak Hasan, for their invaluable guidance, continuous support, and insightful feedback throughout the duration of this study. Their expertise and encouragement have been instrumental in shaping this research and pushing it towards excellence. We are also grateful to the members of our research team, Putri ZURIATI, whose dedication, and hard work significantly contributed to the execution of experiments, data analysis, and discussions, enriching the quality of this work. Furthermore, we acknowledge the support

provided by the Teuku Umar University, including the resources, facilities, and funding that facilitated the smooth progress of this research project. We extend our appreciation to all individuals and organizations who generously helped, resources, and expertise essential for the completion of this study. I wish to express gratitude for the financial assistance provided by Internal Research Grant was funded in June 2022 by LPPM – Teuku Umar University under contract number 013/UN59.7/SPK-PPK/06, which significantly facilitated the experimental work and acquisition of necessary materials. Additionally, heartfelt thanks go to my family and friends for their constant support and understanding throughout the demanding phases of this research project. Lastly, we would like to express our heartfelt thanks to our families and friends for their unwavering support, understanding, and encouragement throughout this academic journey. Without the collective efforts and support of all mentioned above, this research would not have been possible. Thank you all for your invaluable contributions.

References

- [1] Li Z, Zhou X, Ma H, Hou D. Advanced concrete technology. John Wiley & Sons; 2022. <https://doi.org/10.1002/9781119806219>
- [2] Setareh M, Darvas R. Concrete structures. Springer; 2007.
- [3] Zhong K, Zhou J, Zhao C, Yun K, Qi L. Effect of interfacial transition layer with CNTs on fracture toughness and failure mode of carbon fiber reinforced aluminum matrix composites. *Compos. Part Appl. Sci. Manuf.* 2022;163:107201. <https://doi.org/10.1016/j.compositesa.2022.107201>
- [4] Abou-Zeid M, et al. Control of cracking in concrete structures. *Rep ACI Comm.* 2001;224:12-16.
- [5] Paul SC, van Zijl GP, Šavija B. Effect of fibers on durability of concrete: A practical review. *Materials.* 2020;13(20):4562. <https://doi.org/10.3390/ma13204562>
- [6] Wang L, et al. The influence of fiber type and length on the cracking resistance, durability and pore structure of face slab concrete. *Constr. Build. Mater.* 2021;282:122706. <https://doi.org/10.1016/j.conbuildmat.2021.122706>
- [7] Perry JI, Walley SM. Measuring the effect of strain rate on deformation and damage in fibre-reinforced composites: A review. *J. Dyn. Behav. Mater.* 2022;8(2):178-213. <https://doi.org/10.1007/s40870-022-00331-0>
- [8] Nurazzi NM, et al. A review on natural fiber reinforced polymer composite for bullet proof and ballistic applications. *Polymers.* 2021;13(4):646. <https://doi.org/10.3390/polym13040646>
- [9] Hu YT, Ting Y, Hu JY, Hsieh SC. Techniques and methods to study functional characteristics of emulsion systems. *J. Food Drug Anal.* 2017;25(1):16-26. <https://doi.org/10.1016/j.jfda.2016.10.021>
- [10] Qu F, Li W, Dong W, Tam VW, Yu T. Durability deterioration of concrete under marine environment from material to structure: A critical review. *J. Build. Eng.* 2021;35:102074. <https://doi.org/10.1016/j.jobe.2020.102074>
- [11] Sinha S, Devnani GL. Natural fiber composites: processing, characterization, applications, and advancements. CRC Press; 2022. <https://doi.org/10.1201/9781003201724>
- [12] Fan M, Dai D, Huang B. Fourier transform infrared spectroscopy for natural fibres. *Fourier Transform-Mater. Anal.* 2012;3:45-68. <https://doi.org/10.5772/35482>
- [13] Alvarez VA, Vázquez A. Influence of fiber chemical modification procedure on the mechanical properties and water absorption of MaterBi-Y/sisal fiber composites. *Compos. Part Appl. Sci. Manuf.* 2006;37(10):1672-1680. <https://doi.org/10.1016/j.compositesa.2005.10.005>
- [14] Rogers CW. Structures of Building Design Standards: Leveraging Network Analysis to Understand Perceived Complexity [dissertation]. University of Pittsburgh; 2023.

- [15] Shaw A, Sriramula S, Gosling PD, Chryssanthopoulos MK. A critical reliability evaluation of fibre reinforced composite materials based on probabilistic micro and macro-mechanical analysis. *Compos. Part B Eng.* 2010;41(6):446-453. <https://doi.org/10.1016/j.compositesb.2010.05.005>
- [16] Feng Y, Hao H, Lu H, Chow CL, Lau D. Exploring the development and applications of sustainable natural fiber composites: A review from a nanoscale perspective. *Compos. Part B Eng.* 2024;111369. <https://doi.org/10.1016/j.compositesb.2024.111369>
- [17] Fidan I, Naikwadi V, Alkunte S, Mishra R, Tantawi K. Energy Efficiency in Additive Manufacturing: Condensed Review. *Technologies.* 2024;12(2):21. <https://doi.org/10.3390/technologies1202021>
- [18] Gebremariam HG, Taye S, Tarekegn AG. Disparity in research findings on parent concrete strength effects on recycled aggregate quality as a challenge in aggregate recycling. *Case Stud. Constr. Mater.* 2023;19. <https://doi.org/10.1016/j.cscm.2023.e02342>
- [19] Terzić A, et al. The effect of alternations in mineral additives (zeolite, bentonite, fly ash) on physico-chemical behavior of Portland cement based binders. *Constr. Build. Mater.* 2018;180:199-210. <https://doi.org/10.1016/j.conbuildmat.2018.06.007>
- [20] Nurshamila SB, Ismail H, Othman N. The effects of rattan filler loadings on properties of rattan powder-filled polypropylene composites. *BioResources.* 2012;7(4):5677-5690. <https://doi.org/10.15376/biores.7.4.5677-5690>
- [21] Fang H, Bai Y, Liu W, Qi Y, Wang J. Connections and structural applications of fibre reinforced polymer composites for civil infrastructure in aggressive environments. *Compos. Part B Eng.* 2019;164:129-143. <https://doi.org/10.1016/j.compositesb.2018.11.047>
- [22] Yusra A, et al. Effect of the Addition of Natural Fibers on the Mechanical Properties of Concrete. *E3S Web of Conferences.* EDP Sciences; 2024;01027. <https://doi.org/10.1051/e3sconf/202447601027>
- [23] Topić Popović N, Lorencin V, Strunjak-Perović I, Čož-Rakovac R. Shell waste management and utilization: Mitigating organic pollution and enhancing sustainability. *Appl. Sci.* 2023;13(1):623. <https://doi.org/10.3390/app13010623>
- [24] Kim MO, Lee MK. Strength and Microstructural Changes in Cementitious Composites Containing Waste Oyster Shell Powder. *Buildings.* 2023;13(12):3078. <https://doi.org/10.3390/buildings13123078>
- [25] Ahmad R, Hamid R, Osman SA. Physical and chemical modifications of plant fibres for reinforcement in cementitious composites. *Adv. Civ. Eng.* 2019;2019. <https://doi.org/10.1155/2019/5185806>
- [26] C on C Aggregates. Standard test method for compressive strength of cylindrical concrete specimens. *ASTM international*; 2014.
- [27] Nasional BS. SNI 03-1974-1990 Metode Pengujian Kuat Tekan Beton. *Badan Stand. Nas. Indones.*; 1990.
- [28] Waani JE, Elisabeth L. Substitusi material pozolan terhadap semen pada kinerja campuran semen. *J. Tek. Sipil.* 2017;24(3):237-245.
- [29] Durdziński PT, Dunant CF, Haha MB, Scrivener KL. A new quantification method based on SEM-EDS to assess fly ash composition and study the reaction of its individual components in hydrating cement paste. *Cem. Concr. Res.* 2015;73:111-122. <https://doi.org/10.1016/j.cemconres.2015.02.008>
- [30] Georget F, Schmatz J, Wellmann E, Matschei T. A critical catalogue of SEM-EDS multispectral maps analysis methods and their application to hydrated cementitious materials. *J. Microsc.* 2023. <https://doi.org/10.1111/jmi.13245>
- [31] Rollakanti CR, Prasad CVS, Poloju KK, Al Muharbi NMJ, Arun YV. An experimental investigation on mechanical properties of concrete by partial replacement of cement with wood ash and fine sea shell powder. *Mater. Today Proc.* 2021;43:1325-1330. <https://doi.org/10.1016/j.matpr.2020.09.164>

- [32] Hospodarova V, Singovszka E, Stevulova N. Characterization of Cellulosic Fibers by FTIR Spectroscopy for Their Further Implementation to Building Materials. *Am. J. Anal. Chem.* 2018;09(06):303-310. <https://doi.org/10.4236/ajac.2018.96023>
- [33] Rahmawati C, Aprilia S, Saidi T, Aulia TB. Mineralogical, Microstructural and Compressive Strength Characterization of Fly Ash as Materials in Geopolymer Cement. *Elkawnie.* 2021;7(1):1-17. <https://doi.org/10.22373/ekw.v7i1.7787>
- [34] Prasad DD, Ravande K. Fourier transformed-infrared spectroscopy (FTIR) studies on the concrete/cement mortar mass made of cent percentage recycled coarse and fine aggregates. *Int J Adv Res Eng Technol.* 2021;12(1):387-400.
- [35] Zhang D, Yu J, Wu H, Jaworska B, Ellis BR, Li VC. Discontinuous micro-fibers as intrinsic reinforcement for ductile Engineered Cementitious Composites (ECC). *Compos. Part B Eng.* 2020;184:107741. <https://doi.org/10.1016/j.compositesb.2020.107741>
- [36] Harle S, Dhawale V. Comparison of Different Natural Fiber Reinforced Concrete. *Int J Eng Sci Res Technol.* 2014;3:605-607.
- [37] Güneyisi E, Gesoğlu M. Properties of self-compacting portland pozzolana and limestone blended cement concretes containing different replacement levels of slag. *Mater. Struct.* 2011;44:1399-1410. <https://doi.org/10.1617/s11527-011-9706-0>
- [38] Zhao J, Gao X, Chen S, Lin H, Li Z, Lin X. Hydrophobic or superhydrophobic modification of cement-based materials: A systematic review. *Compos. Part B Eng.* 2022;243:110104. <https://doi.org/10.1016/j.compositesb.2022.110104>
- [39] Nduka DO, Akanbi ET, Ojo DO, Babayemi TE, Jolayemi KJ. Investigation of the Mechanical and Microstructural Properties of Masonry Mortar Made with Seashell Particles. *Materials.* 2023;16(6):2471. <https://doi.org/10.3390/ma16062471>
- [40] Committee ACI. State of the Art Report in Fiber Reinforced Concrete. ACI Am. Concr. Inst. Farmington Hills MI USA; 1982.
- [41] Alvee AR, et al. Experimental study of the mechanical properties and microstructure of geopolymer paste containing nano-silica from agricultural waste and crystalline admixtures. *Case Stud. Constr. Mater.* 2022;16 <https://doi.org/10.1016/j.cscm.2021.e00792>
- [42] Mobasher B. Mechanics of fiber and textile reinforced cement composites. CRC press; 2011. <https://doi.org/10.1201/b11181>